Inducing molecular reactions by selective vibrational excitation of a remote antenna with near-infrared light

Cláudio M. Nunes,* Nelson, A. M. Pereira, Luís P. Viegas, Teresa M. V. D. Pinho e Melo, and Rui Fausto

University of Coimbra, CQC, Department of Chemistry, 3004-535 Coimbra, Portugal

Email: cmnunes@qui.uc.pt

Electronic Supplementary Information (ESI)

Table of Contents:

1. Experimental and Computational Methods

Synthesis of 2,6-Difluoro-4-Hydroxyphenylazide:

Commercial reagents were used as purchased. ^{1}H, ^{13}C and ^{19}F Nuclear Magnetic Resonance (NMR) spectra were recorded on an NMR spectrometer Bruker Avance III operating at 400, 100 and 376.5 MHz, respectively. Chemical shifts are referred to the residual signal of DMSO-d_6 or to the internal standard tetramethylsilane (TMS). Chemical shifts are given in parts per million (ppm) relative to TMS and coupling constants *J* are given in Hertz. Thin-layer chromatography (TLC) was carried out on silica gel 60 F_{254} plates (AL TLC 20x20). Column chromatography was performed on Silica Gel 60 (0.04 - 0.063 mm).

The azide **1** was prepared according to an adapted procedure described for other similar derivatives.[S1]

4-Amino-3,5-difluorophenol (300 mg, 2.1 mmol) was dissolved in trifluoroacetic acid (3 ml) and the solution was cooled in an ice bath. Sodium nitrite (171 mg, 2.5 mmol) was added portionwise with stirring over 5 minutes followed by the addition of sodium azide (171 mg, 2.6 mmol). The solution was allowed to stir for an additional 1 h. Then, water (25 ml) was added, and the reaction mixture was extracted with ethyl acetate (3 x 25 ml), washed well with water and saturated aqueous $NaHCO_3$. The extract was dried over anhydrous sodium sulfate and the solvent evaporated *in vacuo* to yield a dark oil. This residue was purified by column chromatography (silica gel; eluent: hexane /ethyl acetate, 3:1) to give, after removing the solvent, the desired azide **1** as a brown oil (180 mg, 51% yield). Exposure to light or kept the product at room temperature results in degradation and, therefore, it should be stored in the dark below room temperature (< −10 ºC) to minimize its decomposition.

^{1}H NMR (400 MHz, DMSO_d_6): δ (ppm) 10.42 (bs, 1H, OH), 6.60-6.53 (m, 2H, Ph-H). ^{13}C NMR (100 MHz, DMSO_d_6): δ (ppm) 155.6 (t, J = 14.0 Hz), 155.5 (dd, J = 245.6, 7.8 Hz), 106.9 (t, J = 15.1 Hz), 100.2-99.9 (m). ^{19}F NMR (376.5 MHz, DMSO_d_6): δ (ppm) −123.12 (s, 2F). IR (Kr matrix, 15 K) wavenumber (cm^{-1}): 621 (w), 651 (w), 704 (vw), 790 (w), 817 (w), 843 (w), 1002 (w), 1049 (s), 1118 (m), 1138 (w), 1144/1145 (w), 1231/1232 (m), 1300/1303 (m), 1321/1327 (br), 1380 (vw), 1462 (w), 1480 (w), 1513 (s), 1516 (w), 1606 (w, H_2O), 1628 (w), 1648 (w), 2083 (w), 2104 (w), 2135 (s), 3626 (m) and 7080 (vw).

Matrix Isolation Spectroscopy: A sample of azide **1** was placed in a glass tube that was then connected to a stainless-steel needle valve (SS4 BMRG valve NUPRO) attached to the vacuum chamber of a cryostat (APD Cryogenics closed-cycle refrigerator with DE-202A expander). For the preparation of the matrices, the sample vapors (at room temperature) were deposited together with a large excess of krypton (N48, Air Liquide) onto a CsI window at 15 K. The temperature was measured directly at the sample holder window by a silicon diode sensor connected to a digital controller (LakeShore 331), providing stabilization accuracy of 0.1 K. Infrared spectra were recorded using a Thermo Nicolet 6700 Fourier transform infrared (FTIR) spectrometer, equipped with a deuterated triglycine sulfate (DGTS) detector and a KBr beam splitter, for the mid-IR range (4000–400 cm^{-1}), or with a thermoelectrically cooled indium gallium arsenide (InGaAs) detector and a CaF_2 beam splitter, for the near-IR range (7500−4000 cm^{-1}). The infrared spectra were recorded with resolution 0.5 and 2 cm^{-1} in the mid-IR and near IR ranges, respectively. Modifications of the sample compartment of the spectrometer were done to accommodate the cryostat head and allow purging of the instrument by a stream of dry air to avoid interference from atmospheric H_2O and CO_2.

Irradiation Experiments: The matrix-isolated species were irradiated through a quartz window of the cryostat, using frequency-tunable narrowband light (full width at half-maximum [FWHM] ≈ 0.2 cm^{-1}) provided by a frequency-doubled signal (UV range), a signal (visible range) or an idler (near-IR range) beam of an optical parametric oscillator (Spectra Physics Quanta-Ray MOPO-SL) pumped with a pulsed Nd:YAG laser (Spectra-Physics PRO-230: output power ≈ 4.3 W; wavelength = 355 nm; duration = 10 ns; repetition rate =10 Hz).

IR Spectra Computations: To support the assignment of the experimental mid-IR spectra, geometry optimizations and harmonic frequency computations were performed at the B3LYP/6-311+G(2d,p) level of theory,[S2–S5] using Gaussian 16 (Revision B.01)[S6] software package. All computations were performed using the tight optimization criteria and an ultrafine integration grid. The nature of stationary points was confirmed by the analysis of the Hessian matrices. In order to correct for the neglected anharmonic effects, incomplete treatment of electron correlation, and basis set limitations, the harmonic vibrational frequencies were scaled by a factor of 0.979.[S7] The scaled harmonic vibrational frequencies

and the respective absolute intensities were used to simulate the IR spectra by convoluting each peak with a Lorentzian function (FWHM = 1 cm^{-1}). In this case, the integral band intensities correspond to the calculated infrared absolute intensities in units of km mol^{-1}.

To support the assignment of the experimental OH stretching fundamentals and first overtones, geometry optimizations and anharmonic frequency computations, using the fully automated generalized second-order vibrational perturbative theory (GVPT2),[S8–S9] were performed at the B3LYP/SNSD[10] level of theory, using Gaussian 16 (Revision B.01). All computations were performed using the very tight optimization criteria and a superfine integration grid.

Computations of the PES: The single-point energy coupled-cluster calculations with singles, doubles, and perturbative triples [CCSD(T)] were performed with the cc-pVTZ basis set[S11] and through the algorithms[S12–S14] present in the GAMESS-US package[S15]. Such calculations were based on geometries optimized at the B3LYP/6-311+G(2d,p) level of theory. Multireference calculations were performed with the CASSCF method[S16–S19] employing an active space consisting of eight electrons and eight orbitals and executed with the cc-pVTZ basis set, hereafter designated CASSCF(8,8)/cc-pVTZ level of theory, using the GAMESS-US package. Following the approach used in the CASSCF calculations of fluorinated derivatives of phenylnitrene,[S20] the eight orbitals included in the active space were selected to be analogous to those used in similar calculations involving the ring expansion of phenylnitrene[S21]. For example, for **2** the (8,8) active space consisted of seven π and π^* molecular orbitals (MOs), plus the in-plane p atomic orbital on nitrogen. For the species **4**, the four π and the four π^* MOs of the double bonds were used. For all transition states and also for **3**, the active space consisted of six MOs mainly π in character plus a $\sigma/\sigma*$ pair. Dynamical correlation was added to the CASSCF results via multireference Møller-Plesset MRMP(8,8)/cc-pVTZ calculations[S22–S25] using the geometries previously optimized at the CASSCF(8,8)/cc-pVTZ level of theory.

Tunneling Rates Computations: Tunneling computations were performed based on B3LYP/6-311+G(2d,p) computed potential energy profiles along the intrinsic reaction coordinate (IRC) in non-mass-weighted Cartesian coordinates (expressed in units of Bohr).[S26] The transmission coefficients for H-atom tunneling through a parabolic barrier

were computed using the Wentzel−Kramers−Brillouin (WKB) approximation.[S27–S29] Accordingly, the probability *P(E)* of tunneling is given by equation (1):[S30]

$$P(E) = e^{-\pi^2 w\sqrt{2m(V_0-E)}/h} \qquad (1)$$

where a particle with mass *m* tunnels through a barrier with height V_0 and width *w*, (V_0–*E*) is the energy deficiency of the particle with respect to the top of the barrier, and *h* is the Planck's constant. For the OH-rotamerization **3a→3s**, the computed probability of tunneling was estimated equal to 4.8×10^{-6}, using the calculated barrier height of 7.8 kJ mol^{-1} (1.9 kcal mol^{-1}) and width at the ZPVE level of 2.37 Bohr (Figure S6). The tunneling rate is the product of the probability of tunneling (transmission coefficient) and the frequency of attempts. If the H-atom of the OH moiety of **3a** is vibrating at a τ(OH) torsional frequency of about 214 cm^{-1} [B3LYP/6-311+G(2d,p) computed value] this results in a tunneling rate of 3.1×10^{7} s^{-1}, *i.e.* a half-life time of 2.3×10^{-8} s. For the OH-rotamerization **4s→4a**, the computed probability of tunneling was estimated equal to 5.1×10^{-10}, using the calculated barrier height of 16.0 kJ mol^{-1} (3.8 kcal mol^{-1}) and width at the ZPVE level of 2.89 Bohr (Figure S7). If the H-atom of the OH moiety of **4s** is vibrating at a τ(OH) torsional frequency of about 348 cm^{-1} [B3LYP/6-311+G(2d,p) computed value], this results in a tunneling rate of 5.3×10^{3} s^{-1}, *i.e.* a half-life time of 1.3×10^{-4} s.

2. Figures

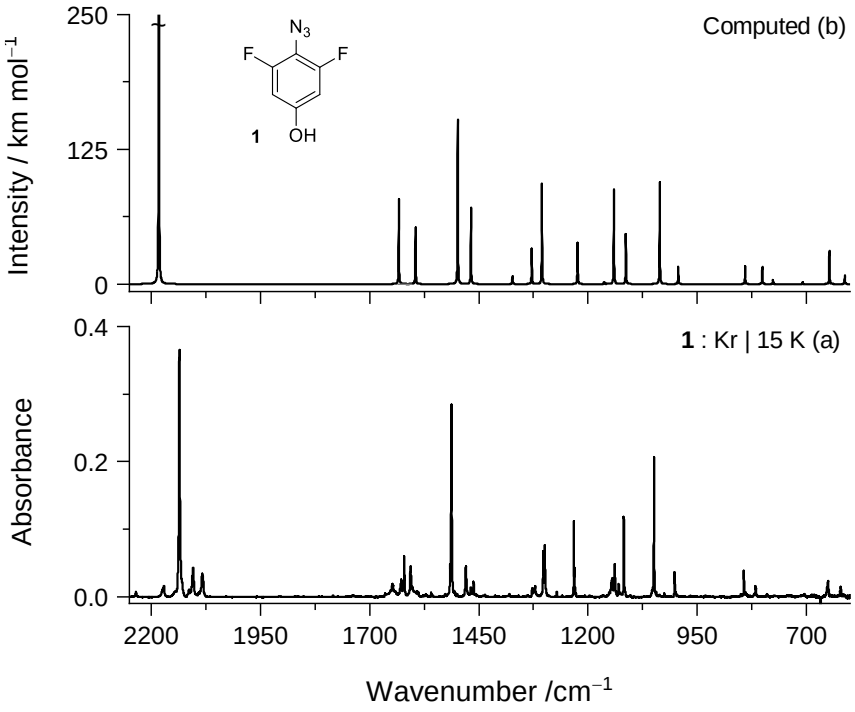

Figure S1. (a) Experimental IR spectrum of azide **1** isolated in a Kr matrix at 15 K. (b) B3LYP/6-311+G(2d,p) computed IR spectrum of azide **1**. Selected regions of the near-IR and mid-IR spectra showing the 2ν(OH) and ν(OH) modes of **1** are provided in Figure S3.

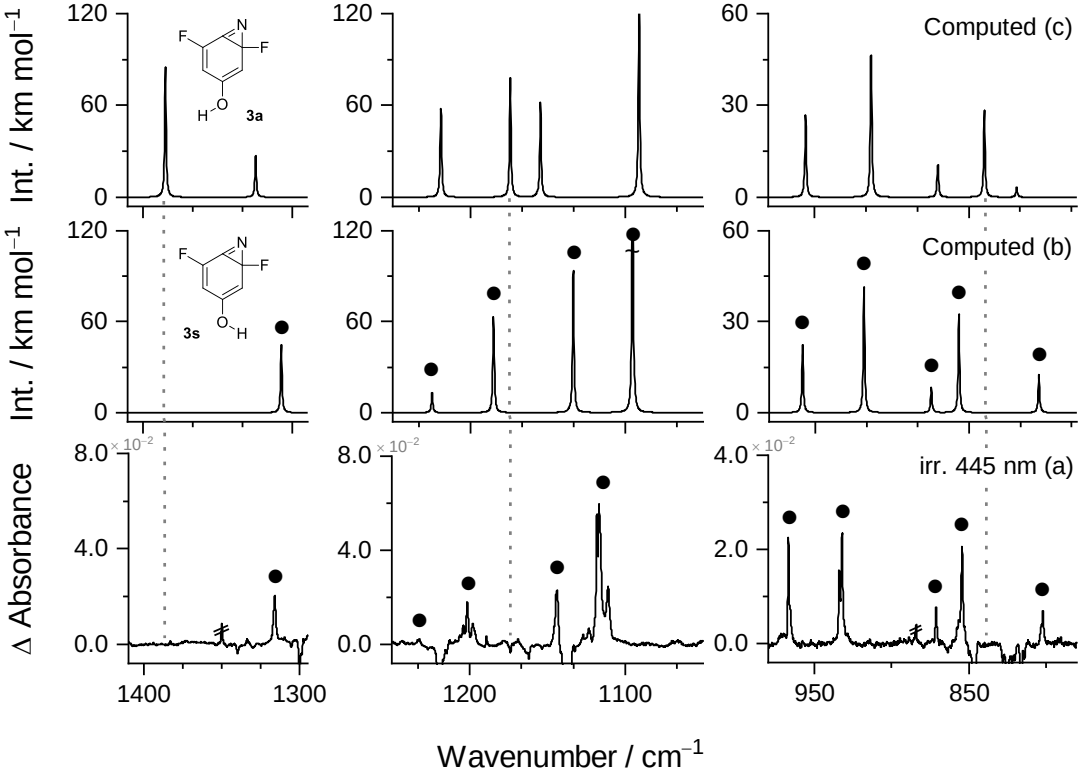

Figure S2. (a) Experimental difference IR spectrum showing changes after irradiation of triplet nitrene ^{3}**2** at 445 nm (50 min, 100 mW, Kr matrix at 15 K). The upward bands signed with closed circles (●) are due to the produced benzazirine **3s**. The upward bands signed with double line are due to a minor amount of an unidentified product. (b,c) B3LYP/6-311+G(2d,p) computed IR spectra of *syn*-OH **3s** and *anti*-OH **3a**. Vertical dotted lines indicate the absence of distinctive computed IR bands of **3a** in the experimental IR spectrum.

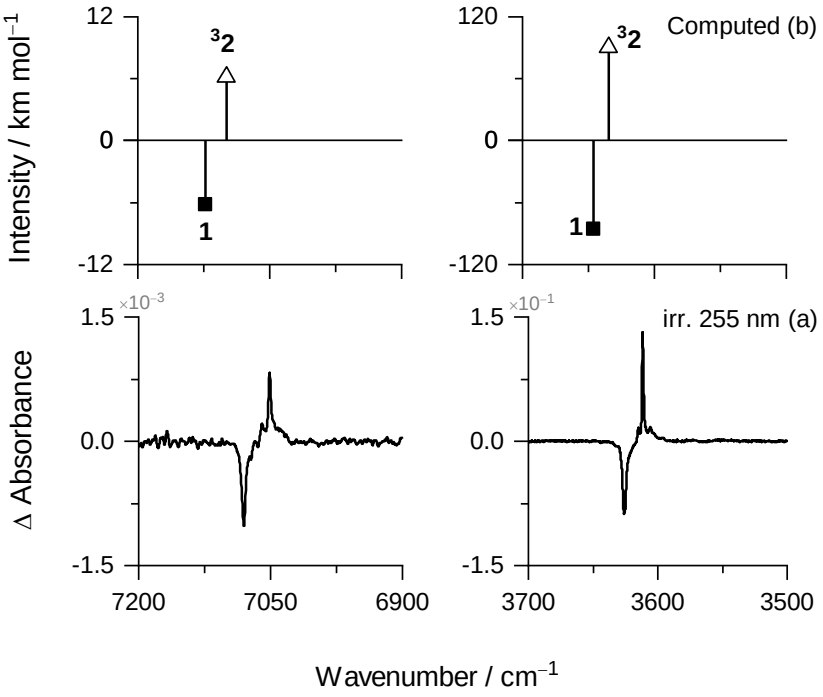

Figure S3. (a) Selected regions of the experimental difference near-IR (left) and mid-IR (right) spectra showing changes resulting from irradiation of azide **1** at 255 nm (8 min, 30 mW, Kr matrix at 15 K). (b) Anharmonic wavenumbers and IR intensities computed at the B3LYP/SNSD level for the 2ν(OH) (left) and ν(OH) (right) modes of azide **1** (squares, intensities multiplied by −1) and of triplet nitrene ^{3}**2** (triangles).

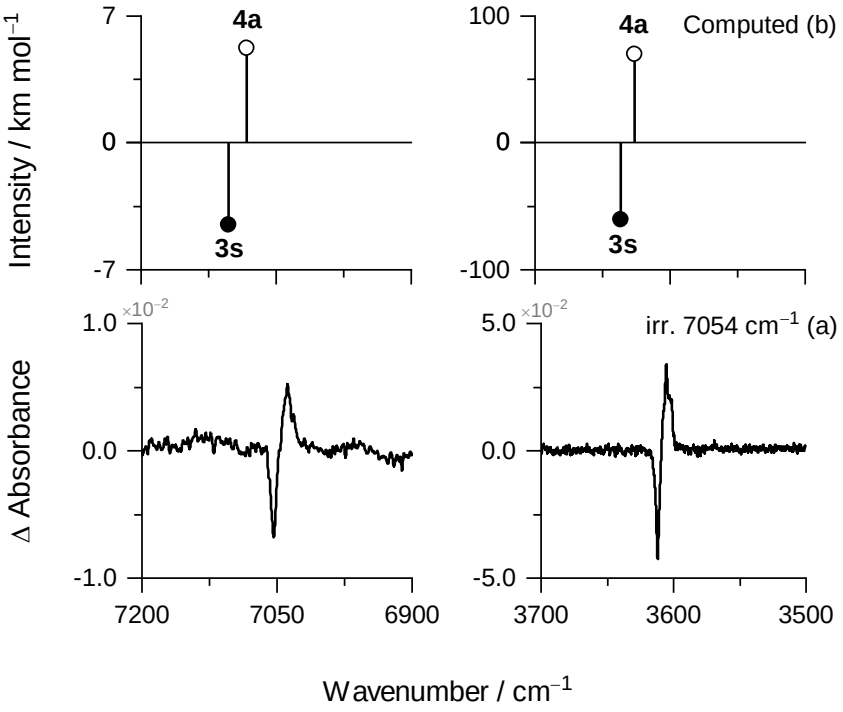

Figure S4. (a) Selected regions of the experimental difference near-IR (left) and mid-IR (right) spectra showing changes resulting from irradiation of benzazirine **3s** at 7054 cm^{-1} (30 min, 100 mW, Kr matrix at 15 K). (b) Anharmonic wavenumbers and IR intensities computed at the B3LYP/SNSD level for the 2ν(OH) (left) and ν(OH) (right) modes of benzazirine **3s** (closed circles, intensities multiplied by −1) and of cyclic ketenimine **4a** (open circles).

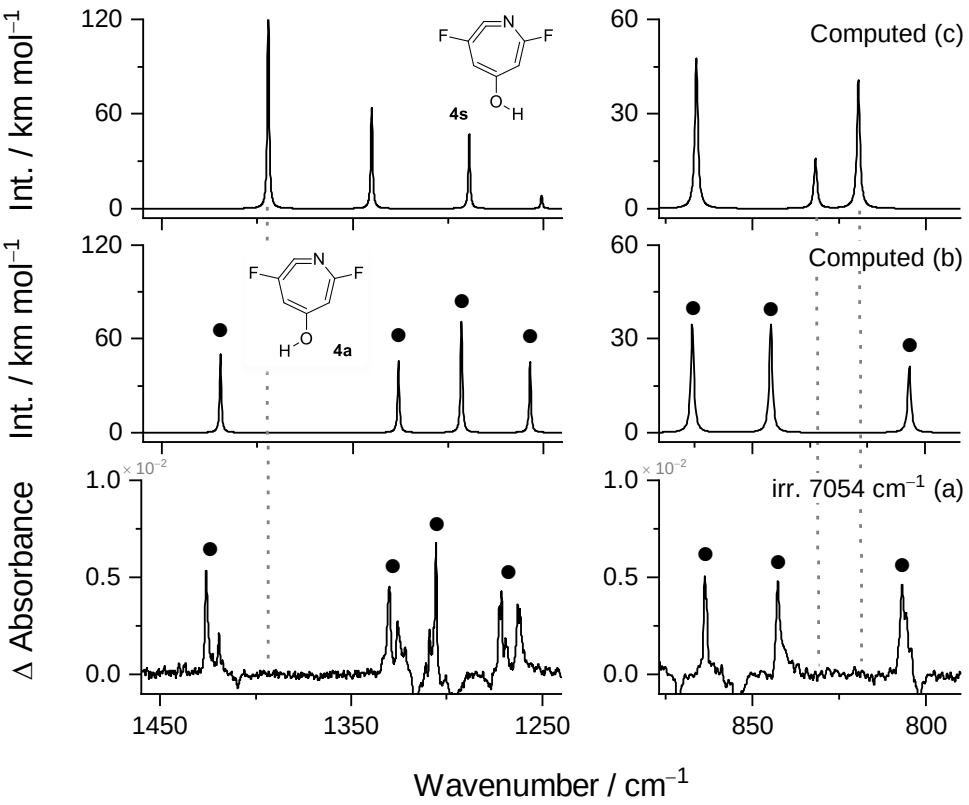

Figure S5. (a) Experimental difference IR spectrum showing changes after irradiation of benzazirine **3s** at 7054 cm^{-1} (30 min, 100 mW, Kr matrix at 15 K). The upward bands signed with closed circles (●) are due to the produced cyclic ketenimine **4a**. (b,c) B3LYP/6-311+G(2d,p) computed IR spectra of *anti*-OH **4a** and *syn*-OH **4s**. Vertical dotted lines indicate the absence of distinctive computed IR bands of **4s** in the experimental IR spectrum.

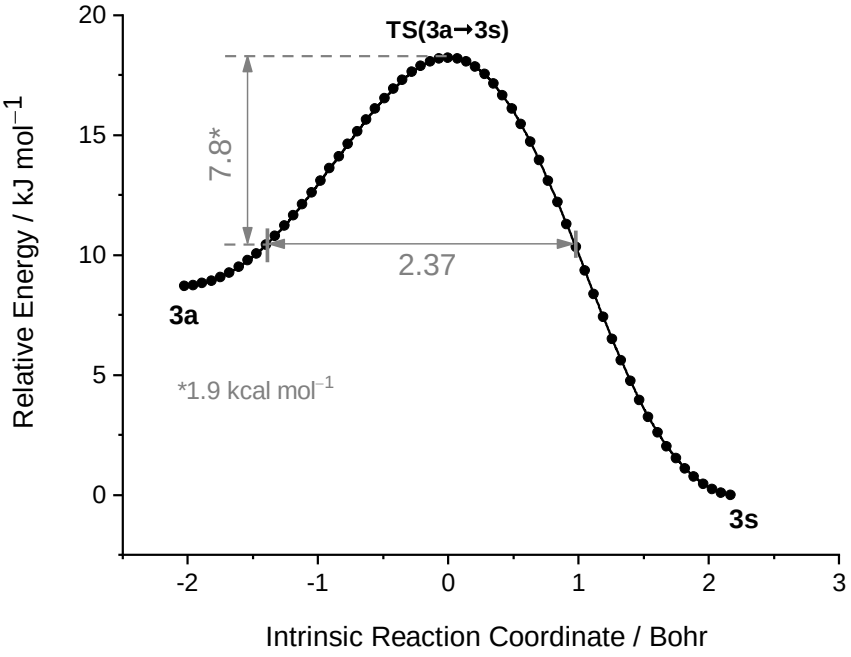

Figure S6. Relative electronic energy as a function of intrinsic reaction coordinate (IRC) for OH-rotamerization of **3a** to **3s** computed at the B3LYP/6-311+G(2d,p) level in non-mass-weighted (Cartesian) coordinates. The vertical arrow designates the B3LYP/6-311+G(2d,p) ZPVE-corrected energy of the reactant **3a** relative to the transition state **TS(3a→3s)** [a similar value was computed at CCSD(T)/cc-pVTZ//B3LYP/6-311+G(2d,p) level, see Figure 4]. The horizontal arrow designates the barrier width considering the ZPVE-corrected energy values of the stationary points superimposed with the pure electronic IRC energy profile.

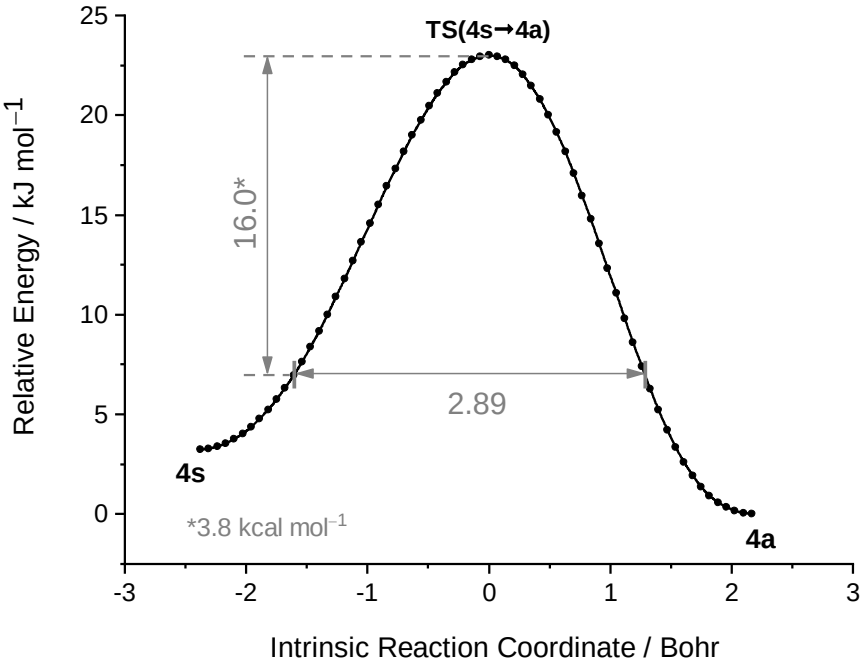

Figure S7. Relative electronic energy as a function of intrinsic reaction coordinate (IRC) for OH-rotamerization of **4s** to **4a** computed at the B3LYP/6-311+G(2d,p) level in non-mass-weighted (Cartesian) coordinates. The vertical arrow designates the B3LYP/6-311+G(2d,p) ZPVE-corrected energy of the reactant **4s** relative to the transition state **TS(4s→4a)** [a similar value was computed at CCSD(T)/cc-pVTZ//B3LYP/6-311+G(2d,p) level, see Figure 4]. The horizontal arrow designates the barrier width considering the ZPVE-corrected energy values of the stationary points superimposed with the pure electronic IRC energy profile.

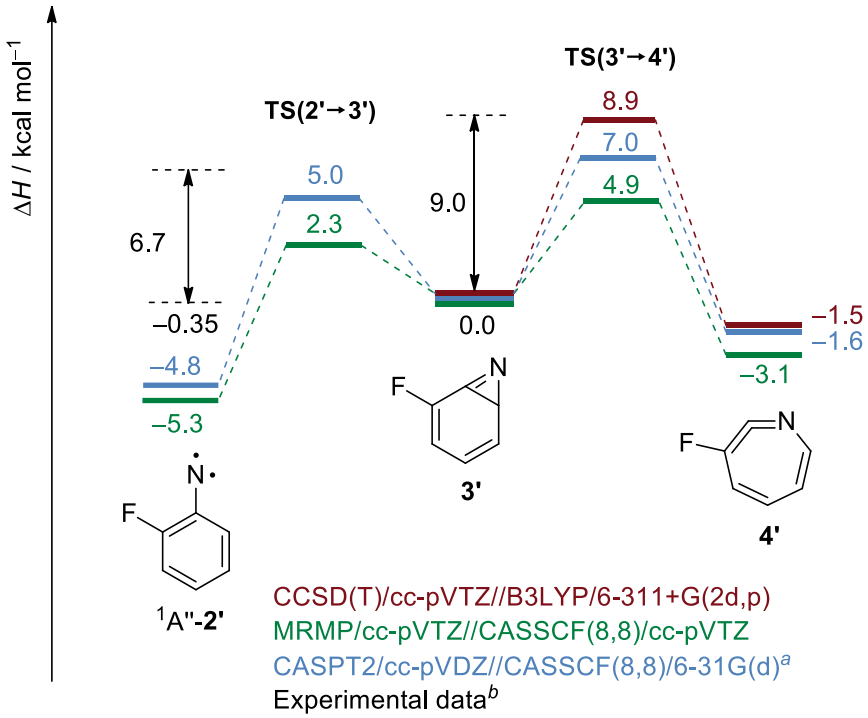

Figure S8. Reaction pathways for 2-fluoro-2*H*-benzazirine **3'** computed at CCSD(T)/cc-pVTZ//B3LYP/6-311+G(2d,p) + ZPVE (red) and MRMP/cc-pVTZ//CASSCF(8,8)/cc-pVTZ + ZPVE (green) levels of theory. ^{1}A" = open-shell singlet state. [a]Computed data at CASPT2/cc-pVDZ//CASSCF(8,8)/6-31G(d) + ZPVE (blue) level of theory were taken from ref. S20. [b]The experimental data refers to results obtained from laser flash photolysis experiments taken from ref. S20; the activation energies were measured using Arrhenius plots and the energy difference between **2'** and **3'** was obtained from an estimated equilibrium constant. Note that this PES is rather unusual because the **TS(2'→3')** is less energetic than **TS(3'→4')**, and therefore, it allowed the measurement of the activation energy for the ring-expansion of a benzazirine to a cyclic ketenimine (see ref. S20).

3. Nuclear Magnetic Resonance Spectra.

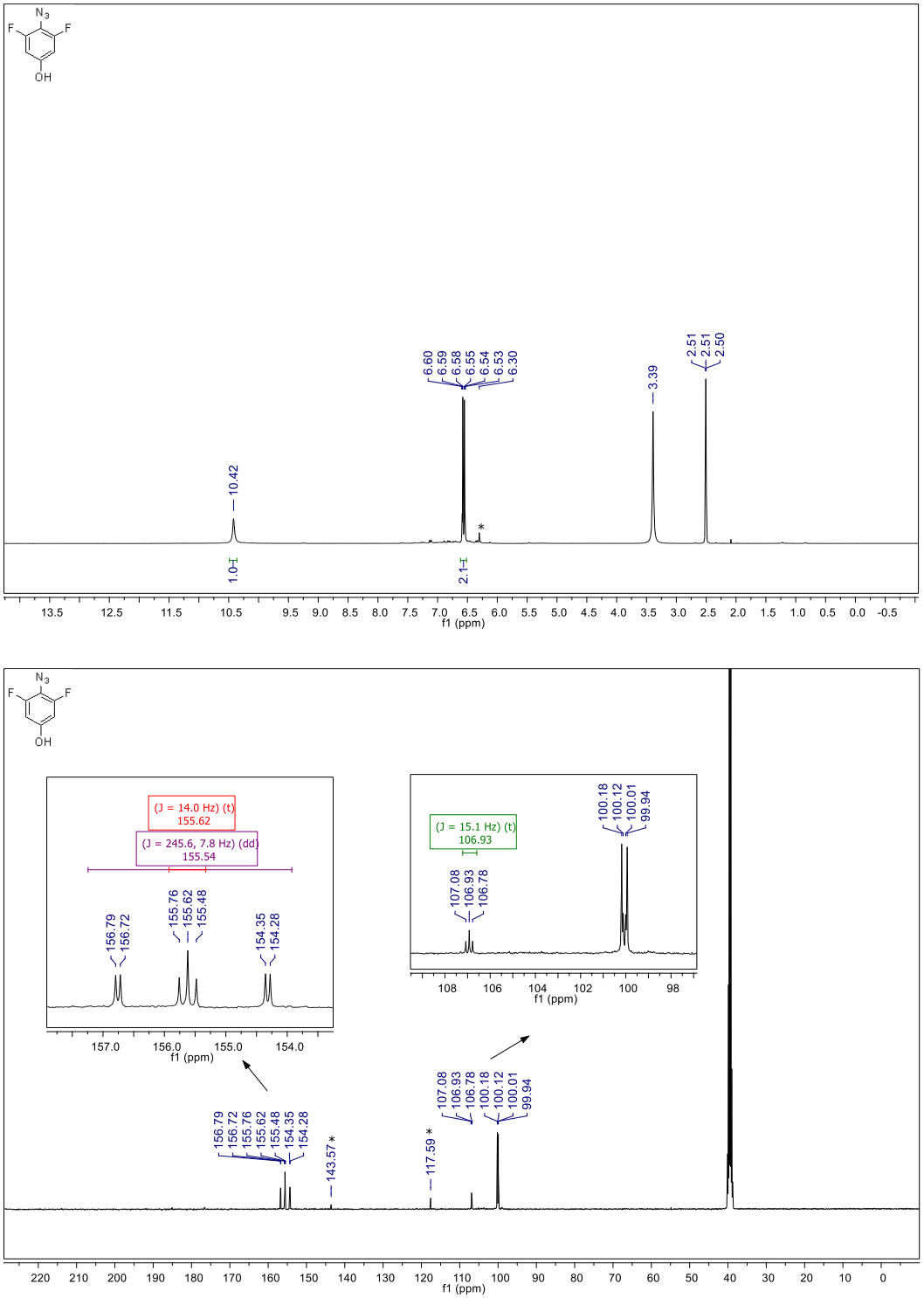

Figure S9a. ^{1}H (upper) and ^{13}C (down) NMR spectra of 2,6-difluoro-4-hydroxyphenylazide (**1**) in DMSO-d_6. *These traces of contaminants should have resulted due to instability of azide **1** under the room temperature conditions of the NMR experiments.

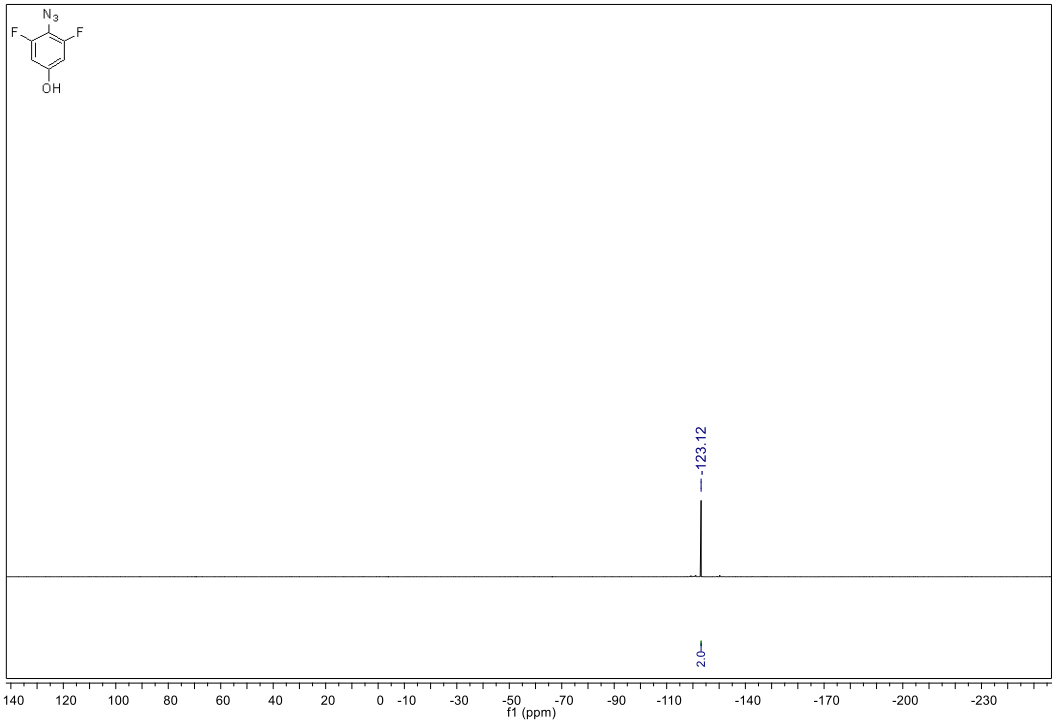

Figure S9b. ^{19}F NMR spectra of 2,6-difluoro-4-hydroxyphenylazide (**1**) in DMSO-d_6.

4. Tables

Table S1. Experimental IR spectral data (krypton matrix at 15 K), B3LYP/6-311+G(2d,p) calculated vibrational frequencies (ν, cm^{-1}), absolute infrared intensities (A^{th}, km mol^{-1}), and vibrational assignment of triplet 2,6-difluoro-4-hydroxyphenylnitrene ^{3}**2**.[a]

Kr matrix[b]		Calculated[c]		Approx. assignment[e]
ν	I	ν	A^{th}	
7051	vw	7099[d]	6.1[d]	[2ν(OH)]
3612	s	3634[d]	90.7[d]	[ν(OH)]
-	-	3143	1.4	[ν(CH)1]
-	-	3115	0.6	[ν(CH)2]
1602/1599	s/m	1598	338.9	[$\nu(CC_{ring})$1]
1536	w	1531	44.7	[$\nu(CC_{ring})$2]
1468	s	1453	150.8	[$\nu(CC_{ring})$3]
1421	w	1409	25.9	[$\nu(CC_{ring})$4]
-	-	1322	0.01	$[\nu(CF)]_s$
1300	w	1291	67.0	[δ(OH)]
1289	w	1273	41.6	[ν(C−N)]
1220/1218	s/w	1206	114.6	[δ(CH)1] + [δ(CH)2]; [δ(OH)]
1162	vw	1159	7.8	[δ(CH)2)]; [δ(OH)]
1139/1137	s/m	1134	236.0	[ν(C−O)]; [δ(CH)1]; [δ(OH)]
1018	s	1007	111.9	$[\nu(CF)]_{as}$
994	w	985	16.6	[$\nu(CC_{ring})$5]
846	w	843	28.3	[γ(CH)1]
825	w	811	25.4	[γ(CH)2]
816	vw	806	13.1	[δ(ring)1]
706	vw	713	4.2	[τ(ring)1]
620	vw	614	11.6	[δ(ring)2]
612	vw	606	8.7	[γ(CH)1] + [γ(CH)2]
-	-	565	0.01	[$\nu(CC_{ring})$6]
-	-	550	1.9	[τ(ring)2]
502	w	500	10.6	[δ(ring)3]

[a]Triplet 2,6-difluoro-4-hydroxyphenylnitrene ^{3}**2** was generated by UV-irradiation (λ = 255 nm) of 2,6-difluoro-4-hydroxyphenylazide **1** in a krypton matrix at 15 K. [b]Experimental intensities are presented in qualitative terms: s = strong, m = medium, w = weak and vw = very weak. [c]B3LYP/6-311+G(2d,p) calculated frequencies scaled by a factor of 0.979. [d] B3LYP/SNSD computed anharmonic vibrational frequencies and absolute IR intensities were given for the 2ν(OH) and ν(OH) modes. [e]Assignments made by inspection of Chemcraft[S31] animation. Abbreviations: ν = stretching, δ = in-plane bending, γ = ou-of-plane bending, τ = torsion, s = symmetric, and as = antisymmetric, ring = 6-member ring. Signs "+" and "–" designate combinations of vibrations occurring in "syn"-phase ("+") and in "anti"-phase ("–").

Table S2. Experimental IR spectral data (krypton matrix at 15 K), B3LYP/6-311+G(2d,p) calculated vibrational frequencies (ν, cm^{-1}), absolute infrared intensities (A^{th}, km mol^{-1}), and vibrational assignment of *syn*-2,6-difluoro-4-hydroxy-2*H*-benzazirine **3s**.[a]

Kr matrix[b]		Calculated[c]		Approx. assignment[e]
ν	I	ν	A^{th}	
7054	vw	7103[d]	4.5[d]	[2ν(OH)]
3612	m	3636[d]	60.8[d]	[ν(OH)]
3075	vw	3130	4.2	[ν(CH)1]
		3100	7.4	[ν(CH)2]
1685	w	1704	63.7	[ν(C=N)]
1620	s	1614	218.3	[ν(C=C_{ring})1]
1546	w	1523	87.1	[ν(C=C_{ring})2]
1410	vw	1417	16.8	[δ(OH)]
1316	s	1308	71.8	[δ(CH)1]; [ν(CC_{ring})3]
1277	vw	1276	28.0	[δ(CH)2]; [ν(C−O)
1232	w	1225	21.4	[ν(CC_{ring})4]; [δ(OH)] – [δ(CH)1]
1201	m	1185	99.5	[ν(CF)1; [δ(OH)] + [δ(CH)2]
1144	m	1134	150.1	[ν(C−O)]; [δ(CH)2] + [δ(CH)1] + [δ(OH)]
1118/1117/1111	m/m/m	1095	265.5	[ν(CF)2]; [δ(CH)2]
967	m	958	35.0	[ν(CC_{ring})5]
934/932	m/m	918	67.9	[ν(CC_{ring})6]
871	vw	875	13.6	[γ(CH)1]
854	m	857	51.0	[γ(CH)1] + [γ(CH)2]
802	w	805	19.6	[γ(CH)2] – [γ(CH)1]
750	vw	748	7.5	[γ(CH)2]
628	vw	629	14.1	[τ(ring)1]
609	vw	608	12.8	[τ(ring)2]
-	-	590	0.1	[δ(ring)1]
533	vw	534	7.2	[δ(ring)2]
501	vw	497	7.9	[δ(ring)3]

[a] *syn*-2,6-Difluoro-4-hydroxy-2*H*-benzazirine **3s** was generated by irradiation (λ = 445 nm) of triplet 2,6-difluoro-4-hydroxyphenylnitrene ^{3}**2** in a krypton matrix at 15 K. [b] Experimental intensities are presented in qualitative terms: s = strong, m = medium, w = weak and vw = very weak. [c] B3LYP/6-311+G(2d,p) calculated frequencies scaled by a factor of 0.979. [d] B3LYP/SNSD computed anharmonic vibrational frequencies and absolute IR intensities were given for the 2ν(OH) and ν(OH) modes. [e] Assignments made by inspection of Chemcraft[S31] animation. Abbreviations: ν = stretching, δ = in-plane bending, γ = ou-of-plane bending, τ = torsion, s = symmetric, and as = antisymmetric, ring = 6-member ring. Signs "+" and "–" designate combinations of vibrations occurring in "syn"-phase ("+") and in "anti"-phase ("–").

Table S3. Experimental IR spectral data (krypton matrix at 15 K), B3LYP/6-311+G(2d,p) calculated vibrational frequencies (ν, cm^{-1}), absolute infrared intensities (A^{th}, km mol^{-1}), and vibrational assignment of *anti*-3,7-difluoro-5-hydroxy-1-aza-1,2,4,6-cycloheptatetraene **4a**.[a]

Kr matrix[b]		Calculated[c]		Approx. assignment[e]
ν	I	ν	A^{th}	
7038	vw	7082[d]	5.2[d]	[2ν(OH)]
3605	m	3626[d]	70.1[d]	[ν(OH)]
-	-	3126	1.7	[ν(CH)1]
-	-	3056	14.6	[ν(CH)2]
1823	br	1856	68.7	$[\nu(C{=}C{=}N)_{as}]$
1592/1584	m/w	1581	273.0	$[\nu(C{=}C_{ring})]_{as}$
1542/1536	w/m	1525	238.3	$[\nu(C{=}C_{ring})]_{s}$
1426/1419	w/vw	1419	79.1	[δ(OH)]; $[\nu(CC_{ring})1]$; [δ(CH)2]
1330/1326	w/vw	1326	72.6	[δ(CH)1]
1309/1306	vw/w	1293	113.1	$[\nu(C{=}C{=}N)]_{s}$
1271/1263	w/w	1257	71.3	$[\nu(CC_{ring})2]$; [δ(OH)]
1217	m	1196	244.6	$[\nu(CF)]_{as}$
1184	vw	1178	51.1	[δ(CH)2]; [δ(OH)]
1139	s	1133	261.3	[ν(C−O)]
992	w	984	47.8	$[\nu(CC_{ring})3]$
879	vw	915	15.3	[ν(CN)]
864	w	867	55.4	[δ(ring)1]
843	w	845	54.4	[γ(CH)1]
807	w	805	34.1	[γ(CH)2]
672	w	680	40.6	[τ(ring)1]
654	vw	660	2.5	[γ(CH)1] + [γ(CH)2]
613	vw	613	12.5	[τ(ring)2]
587	vw	585	4.1	[δ(ring)2]

[a] *anti*-3,7-Difluoro-5-hydroxy-1-aza-1,2,4,6-cycloheptatetraene **4a** was generated in a krypton matrix at 15 K by vibrational excitation of *syn*-2,6-difluoro-4-hydroxy-2*H*-benzazirine **3s** at the 2ν(OH) frequency (7054 cm^{-1}). [b] Experimental intensities are presented in qualitative terms: s = strong, m = medium, w = weak, vw = very weak and br = broad. [c] B3LYP/6-311+G(2d,p) calculated frequencies scaled by a factor of 0.979. [d] B3LYP/SNSD computed anharmonic vibrational frequencies and absolute IR intensities were given for the 2ν(OH) and ν(OH) modes [e] Assignments made by inspection of Chemcraft[S31] animation. Abbreviations: ν = stretching, δ = in-plane bending, γ = ou-of-plane bending, τ = torsion, s = symmetric, and as = antisymmetric, ring = 7-member ring. Signs "+" and "–" designate combinations of vibrations occurring in "syn"-phase ("+") and in "anti"-phase ("–").

Table S4. Single-point energies, in Hartree, of the different structures optimized in this work, calculated with CCSD(T) and MRMP(8,8). Both sets of calculations employ the cc-pV*T*Z basis set and are based on B3LYP/6-311+G(2d,p) and CASSCF(8,8)/cc-pV*T*Z geometries, respectively.

Structure	CCSD(T)	MRMP(8,8)
^{1}A″-**2**	-	-559.0606994439
TS(2 → 3s)	-	-559.0457065027
3a	-559.1448326889	-559.0557473358
TS(3a → 3s)	-559.1412854746	-559.0521492235
3s	-559.1483123697	-559.0592186267
TS(3s → 4s)	-559.1303357690	-559.0494607606
4s	-559.1526596941	-559.0684274228
TS(4s → 4a)	-559.1454870607	-559.0625230406
4a	-559.1538999383	-559.0696783155
^{1}A″-**2′**	-	-384.8106354017
TS(2′ → 3′)	-	-384.7984329120
3′	-384.8823857135	-384.8039036139
TS(3′ → 4′)	-384.8665505346	-384.7945828973
4′	-384.8848588502	-384.8090043445

5. Computational Data

Optimized geometries (Cartesian coordinates, Å), electronic energies (*E*, E_h) and zero-point vibrational energy (ZPVE, E_h) computed at the B3LYP/6-311+G(2d,p), B3LYP/SNSD and CASSCF(8,8)/cc-pVTZ levels of theory.

1s: B3LYP/6-311+G(2d,p) (*E* = -669.733529; ZPVE = 0.090592)

C	-2.208318	-0.371389	-0.000005
C	-1.230131	-1.362169	-0.000006
C	0.099553	-0.985178	0.000000
C	0.523014	0.343697	0.000006
C	-0.502779	1.297570	0.000008
C	-1.842009	0.972171	0.000003
O	-3.542049	-0.653230	-0.000010
H	-3.680472	-1.607201	-0.000014
N	1.845444	0.813845	0.000014
N	2.805240	0.037291	-0.000005
N	3.791030	-0.511664	-0.000018
H	-1.476628	-2.416842	-0.000011
F	1.039822	-1.954547	-0.000001
F	-0.155820	2.593801	0.000015
H	-2.590530	1.752083	0.000004

1a: B3LYP/6-311+G(2d,p) (*E* = -669.733632; ZPVE = 0.090622)

C	-2.201657	-0.403510	-0.000005
C	-1.213286	-1.383571	-0.000004
C	0.108349	-0.991760	0.000002
C	0.521014	0.344510	0.000007
C	-0.510722	1.286344	0.000006
C	-1.849344	0.944146	0.000000
O	-3.497744	-0.825982	-0.000010
H	-4.093873	-0.068430	-0.000011
N	1.839215	0.826059	0.000016
N	2.806093	0.058087	-0.000006
N	3.797145	-0.481097	-0.000022
H	-1.469378	-2.433898	-0.000007
F	1.062582	-1.946338	0.000006
F	-0.183290	2.588465	0.000011
H	-2.591690	1.732738	0.000000

^{3}**2**: B3LYP/6-311+G(2d,p) (*E* = -560.173662; ZPVE = 0.079089)

C	-1.611652	-0.043556	0.000080
C	-0.948869	1.190021	0.000039
C	0.422972	1.207048	-0.000026
C	1.226334	0.025446	-0.000052
C	0.476630	-1.194682	-0.000017
C	-0.890869	-1.244342	0.000049
O	-2.964322	-0.141646	0.000140
H	-3.366145	0.735397	0.000152
N	2.546210	0.056633	-0.000120
H	-1.490993	2.128096	0.000056
F	1.060193	2.384056	-0.000068
F	1.173995	-2.336457	-0.000044
H	-1.406717	-2.194774	0.000077

3s: B3LYP/6-311+G(2d,p) (*E* = -560.145129; ZPVE = 0.079799)

C	1.415117	0.354313	0.029620
C	1.037688	-1.040362	-0.147855
C	-0.250653	-1.437523	-0.079900
C	-1.142661	-0.372838	0.240472
C	-0.881769	1.030429	0.046719
C	0.527698	1.383788	0.119408
O	2.768856	0.514845	0.064725
H	2.986353	1.449031	0.169869
N	-1.640590	0.369985	1.152597
H	1.830617	-1.767393	-0.271817
F	-0.646302	-2.699111	-0.268405
F	-1.639275	1.775222	-0.826632
H	0.853973	2.417870	0.120518

3a: B3LYP/6-311+G(2d,p) (*E* = -560.141810; ZPVE = 0.079367)

C	-1.319728	-0.628465	0.034948
C	-1.212216	0.813414	-0.139938
C	-0.022916	1.453586	-0.073571
C	1.055919	0.581265	0.243337
C	1.064615	-0.849274	0.041994
C	-0.248376	-1.465822	0.108991
O	-2.571237	-1.172916	0.077390
H	-3.244788	-0.485242	0.042933
N	1.671864	-0.061596	1.158908
H	-2.114701	1.400226	-0.276807
F	0.118716	2.766343	-0.277878
F	1.960078	-1.431866	-0.820900
H	-0.386596	-2.538998	0.096826

TS(3a→3s): B3LYP/6-311+G(2d,p) (*E* = -560.138181; ZPVE = 0.078698)

C	-1.399123	-0.403731	0.020159
C	-1.067978	1.003090	-0.149680
C	0.207602	1.446879	-0.075767
C	1.126532	0.412290	0.258479
C	0.919228	-1.004284	0.046190
C	-0.479334	-1.401997	0.087893
O	-2.749347	-0.703005	-0.018636
H	-3.122338	-0.684532	0.870482
N	1.623570	-0.325993	1.173116
H	-1.881599	1.703300	-0.293749
F	0.567997	2.717690	-0.277379
F	1.718631	-1.716287	-0.812509
H	-0.787481	-2.438880	0.045889

TS(3a→3s)': B3LYP/6-311+G(2d,p) (*E* = -560.137643; ZPVE = 0.078712)

C	-1.413398	-0.349231	0.047984
C	-1.027451	1.044253	-0.129378
C	0.265764	1.436947	-0.086249
C	1.150342	0.368179	0.232313
C	0.879379	-1.037954	0.047991
C	-0.533920	-1.380352	0.133270
O	-2.773577	-0.576007	0.161628
H	-3.161999	-0.732605	-0.707181
N	1.645794	-0.378198	1.142941
H	-1.815366	1.781297	-0.225667
F	0.668784	2.695867	-0.280915
F	1.620279	-1.793476	-0.828791
H	-0.880435	-2.405820	0.150994

TS(3s→4s): B3LYP/6-311+G(2d,p) (*E* = -560.131765; ZPVE = 0.077966)

C	-1.064057	-0.975902	0.032203
C	-1.472115	0.366309	0.017164
C	-0.537976	1.392645	0.005843
C	0.690394	1.041024	0.464336
C	1.339071	-0.513240	0.050421
C	0.261554	-1.386035	-0.124391
O	-2.082992	-1.889285	0.063187
H	-1.724134	-2.778828	0.154654
N	1.526660	0.382979	1.147708
H	-2.532472	0.590418	0.004261
F	-0.820109	2.620841	-0.473176
F	2.427229	-0.683614	-0.729039
H	0.468616	-2.362014	-0.551886

4s: B3LYP/6-311+G(2d,p) (*E* = -560.156338; ZPVE = 0.080011)

C	0.288631	1.343384	0.013337
C	1.444824	0.647306	0.257789
C	1.417724	-0.764201	0.042964
C	0.363963	-1.404871	0.513730
C	-1.496560	-0.427636	-0.023515
C	-0.999148	0.798303	-0.347910
O	0.369949	2.698644	0.115598
H	-0.508969	3.093612	0.077492
N	-0.882805	-1.375932	0.752430
H	2.322561	1.174967	0.615502
F	2.421101	-1.384523	-0.617932
F	-2.754814	-0.710849	-0.361274
H	-1.706737	1.478432	-0.810311

4a: B3LYP/6-311+G(2d,p) (*E* = -560.157571; ZPVE = 0.080143)

C	0.345119	1.326420	0.013606
C	1.462447	0.568685	0.264979
C	1.369407	-0.841101	0.049491
C	0.279325	-1.429756	0.501663
C	-1.527056	-0.344827	-0.025630
C	-0.971905	0.857116	-0.337678
O	0.384045	2.684833	0.085352
H	1.289926	2.984708	0.231066
N	-0.961118	-1.333594	0.741902
H	2.373836	1.036062	0.631118
F	2.342374	-1.502372	-0.620010
F	-2.799486	-0.562522	-0.355621
H	-1.638309	1.600536	-0.756222

TS(4s→4a): B3LYP/6-311+G(2d,p) (*E* = -560.149151; ZPVE = 0.078905)

C	0.326104	1.328594	-0.004138
C	1.459350	0.603236	0.231786
C	1.391074	-0.818534	0.053841
C	0.305066	-1.408016	0.511156
C	-1.518748	-0.379193	-0.030821
C	-0.981171	0.828814	-0.354652
O	0.404413	2.711288	0.020431
H	0.338113	3.038897	0.925254
N	-0.930432	-1.330880	0.773758
H	2.370929	1.107829	0.535836
F	2.374878	-1.474609	-0.600618
F	-2.782164	-0.636888	-0.364956
H	-1.655801	1.553198	-0.793714

TS(4s→4a)': B3LYP/6-311+G(2d,p) (*E* = -560.148805; ZPVE = 0.078915)

C	0.338472	1.323150	0.023447
C	1.458013	0.580768	0.272884
C	1.383093	-0.835113	0.052118
C	0.290558	-1.428391	0.484847
C	-1.525080	-0.366226	-0.033543
C	-0.975361	0.844379	-0.331101
O	0.421764	2.695550	0.195100
H	0.597065	3.130922	-0.647681
N	-0.947051	-1.345762	0.738150
H	2.355605	1.071227	0.634715
F	2.367507	-1.477503	-0.616339
F	-2.795979	-0.593990	-0.361542
H	-1.659354	1.585819	-0.725858

1s: B3LYP/SNSD (*E* = -669.563053; ZPVE = 0.091040)

C	2.213765	-0.374333	0.000002
C	1.231458	-1.367174	0.000007
C	-0.101504	-0.986073	0.000005
C	-0.525256	0.347074	-0.000002
C	0.505263	1.301153	-0.000006
C	1.848921	0.974050	-0.000005
O	3.547824	-0.658982	0.000004
H	3.682954	-1.614236	0.000009
N	-1.848371	0.818786	-0.000004
N	-2.807028	0.034843	-0.000001
N	-3.803284	-0.513029	0.000000
H	1.477338	-2.424663	0.000013
F	-1.044639	-1.954716	0.000010
F	0.159298	2.599531	-0.000013
H	2.600091	1.755044	-0.000009

^{3}**2**: B3LYP/SNSD (*E* = -560.034004; ZPVE = 0.079498)

C	-1.617012	-0.044093	0.000075
C	-0.952900	1.193119	0.000038
C	0.423982	1.208489	-0.000027
C	1.230367	0.025645	-0.000059
C	0.478492	-1.195967	-0.000015
C	-0.894239	-1.248169	0.000049
O	-2.970965	-0.142001	0.000140
H	-3.371164	0.736625	0.000154
N	2.555940	0.057404	-0.000120
H	-1.496194	2.133494	0.000058
F	1.061467	2.387667	-0.000063
F	1.176518	-2.339749	-0.000041
H	-1.410501	-2.201350	0.000079

3s: B3LYP/SNSD (*E* = -560.006369; ZPVE = 0.080015)

C	-1.414766	-0.368955	0.029529
C	-1.053377	1.031814	-0.144200
C	0.236543	1.444834	-0.077899
C	1.141885	0.389204	0.240275
C	0.896116	-1.022116	0.047260
C	-0.512476	-1.393179	0.117493
O	-2.767696	-0.547085	0.062679
H	-2.972062	-1.485081	0.167083
N	1.642788	-0.359833	1.154294
H	-1.857037	1.751486	-0.265866
F	0.617804	2.711835	-0.269676
F	1.663955	-1.759289	-0.826768
H	-0.828233	-2.433409	0.110544

4a: B3LYP/SNSD (*E* = -560.016810; ZPVE = 0.080277)

C	0.348173	1.330283	0.015317
C	1.468927	0.566428	0.261346
C	1.367624	-0.844248	0.044245
C	0.275348	-1.439306	0.503395
C	-1.530342	-0.343186	-0.024942
C	-0.971541	0.863811	-0.334904
O	0.392760	2.689781	0.086870
H	1.299741	2.985012	0.240156
N	-0.970874	-1.336289	0.745639
H	2.387297	1.032059	0.620137
F	2.343931	-1.509988	-0.618240
F	-2.804299	-0.556122	-0.360526
H	-1.638824	1.611016	-0.752577

^{1}A"-**2**: CASSCF(8,8)/cc-pVTZ (E=-557.3131157334; ZPVE=0.082895)

N	-0.07805293	-0.95421129	0.30300766
C	-0.10462135	-0.06110994	1.20800960
C	0.94257009	0.08027764	2.22003436
C	0.91560918	1.02960908	3.18318701
C	-1.18568146	0.91547042	1.32841325
C	-1.21714270	1.87033319	2.29359841
C	-0.16808353	1.94358671	3.23646641
H	1.70519233	1.09538090	3.90390420
H	-2.04177141	2.55657220	2.32455564
F	-2.15196514	0.83022094	0.44150713
F	1.93498302	-0.77859491	2.14854765
O	-0.13822268	2.86524677	4.21779156
H	-0.88859618	3.43093729	4.18507814

TS(2→3s): CASSCF(8,8)/cc-pVTZ (E=-557.2958176903; ZPVE=0.083138)

N	0.18680699	-0.00245000	-0.06830007
C	-0.00151827	-0.00441237	1.17469132
C	0.89041013	-0.08134267	2.33695936
C	0.80151004	0.88475788	3.25981855
C	-1.19931710	0.78899795	1.33591688
C	-1.14624429	1.95251787	2.14963293
C	-0.16782099	1.97090292	3.09637618
H	1.46942246	0.92280746	4.09606218
H	-1.89363480	2.71985960	2.08000946
F	-2.32422876	0.46267781	0.75382274
F	1.78184760	-1.03997838	2.39595032
O	0.01012479	2.96882153	3.97603679
H	-0.62796974	3.65050292	3.85769248

3a CASSCF(8,8)/cc-pVTZ (E=-557.3133712354; ZPVE=0.08465)

N	0.28917190	-0.18691537	-0.27148700
C	0.06708919	0.11202268	0.94144785
C	0.63470370	0.00618461	2.26920557
C	1.49755704	0.99354547	2.54908156
C	0.03424222	1.27281952	0.14296862
C	1.14164484	2.20516682	0.38938969
C	1.80312407	2.04541183	1.55543256
H	2.01347971	1.00555968	3.49031305
H	1.37034678	3.01899147	-0.26847419
F	-1.11780405	1.81235683	-0.26012141
F	0.34030885	-0.96991849	3.08941102
O	2.78615499	2.91658163	1.88101852
H	3.39328265	2.54427576	2.49434471

TS(3a→3s): CASSCF(8,8)/cc-pVTZ (E=-557.3116618095; ZPVE=0.084087)

N	-0.01222398	0.54263818	0.06628976
C	0.05670640	-0.01555034	1.20377851
C	0.91680592	-0.17466892	2.35732293
C	0.78791386	0.82357812	3.24378705
C	-1.09270084	0.79538071	1.12503886
C	-1.05918860	1.97303641	2.00572896
C	-0.16216044	1.93371272	3.01300240
H	1.42387772	0.88016927	4.10470676
H	-1.74706697	2.78851724	1.90508258
F	-2.30141234	0.28060868	0.88424993
F	1.76665437	-1.16374958	2.47189021
O	-0.04036412	2.97869420	3.88222337
H	-0.57989019	2.84700346	4.64281893

3s: CASSCF(8,8)/cc-pVTZ (E=-557.3170177567; ZPVE=0.085117)

N	-0.01923295	0.52228433	0.06530289
C	0.05162428	-0.01609785	1.21211958
C	0.91379726	-0.15987955	2.36674666
C	0.78643948	0.84531409	3.24370575
C	-1.09599471	0.79530132	1.12693894
C	-1.05709302	1.98431027	1.98894656
C	-0.15742265	1.95379388	2.99608040
H	1.40842986	0.90829092	4.11368275
H	-1.75791013	2.78933716	1.87440586
F	-2.30569935	0.27827409	0.89535791
F	1.75596344	-1.15290046	2.49787879
O	-0.00465579	2.94104815	3.90280032
H	-0.61470395	3.64071107	3.74915910

TS(3s→4s): CASSCF(8,8)/cc-pVTZ (E=-557.2791207183; ZPVE=0.082933)

N	0.28386357	0.00541881	-0.24431449
C	0.14202280	-0.11984462	1.00616705
C	0.71863389	-0.08015456	2.24375820
C	1.72491920	0.85608548	2.40611124
C	-0.02326079	1.35261226	0.05587316
C	0.93500769	2.25381422	0.52032018
C	1.85650110	1.93057764	1.51847112
H	2.36706901	0.81719333	3.26365376
H	0.85072803	3.27770805	0.20597155
F	-1.15023196	1.81336296	-0.44416466
F	0.25725648	-0.78950328	3.25272584
O	2.87284899	2.78341365	1.80133772
H	3.01025510	3.39363742	1.10039234

4s: CASSCF(8,8)/cc-pVTZ (E=-557.3185958169; ZPVE=0.084995)

N	0.01926215	0.08309273	-0.06613055
C	0.26766476	-0.42877960	1.06142473
C	0.80698276	-0.18761621	2.25294590
C	1.90531003	0.74597025	2.33433676
C	-0.09334650	1.45943987	0.01353359
C	0.70230663	2.27458501	0.73181903
C	1.80249298	1.88865876	1.61895883
H	2.76721668	0.56535161	2.94621634
H	0.57236391	3.32752633	0.56616521
F	-0.98111546	1.97227502	-0.80009234
F	0.33246094	-0.73190856	3.35626364
O	2.79211807	2.80062675	1.75033569
H	2.80163336	3.40728498	1.03246951

TS(4s→4a): CASSCF(8,8)/cc-pVTZ (E=-557.3150612499; ZPVE=0.084082)

N	-0.02161364	0.07647306	-0.05494003
C	0.22899498	-0.43548033	1.07068610
C	0.80150807	-0.21341173	2.24855185
C	1.89948881	0.72591990	2.31915665
C	-0.12627319	1.45710695	0.02460830
C	0.69679248	2.26278329	0.72143865
C	1.80074787	1.86433768	1.59823358
H	2.75191498	0.55019701	2.94685698
H	0.61220586	3.31595063	0.54137850
F	-1.01692855	1.97138429	-0.78548396
F	0.35149005	-0.75878757	3.36189628
O	2.77728915	2.81514287	1.69595647
H	3.53432870	2.57509303	1.19036460

4a: CASSCF(8,8)/cc-pVTZ (E=-557.3201845687; ZPVE=0.085237)

N	-0.03200223	0.07728115	-0.05106344
C	0.22769929	-0.44082871	1.06986272
C	0.80565417	-0.21657120	2.24497914
C	1.91186333	0.70989627	2.30725789
C	-0.11875001	1.45740771	0.02862367
C	0.70336390	2.26113701	0.72774792
C	1.80743051	1.85872388	1.59975719
H	2.77787709	0.50255769	2.90929699
H	0.62581569	3.31369972	0.54258829
F	-1.00540149	1.98091936	-0.77963310
F	0.35074863	-0.75220907	3.36218739
O	2.76078534	2.81258154	1.63133740
H	3.43952918	2.59858084	2.24670291

3': B3LYP/6-311+G(2d,p) (*E* = -385.621481; ZPVE = 0.083466)

C	0.851298	1.498444	-0.177643
C	-0.585045	1.290955	-0.117322
C	-1.101840	0.055567	0.042062
C	-0.104651	-0.973445	0.049654
C	1.300837	-0.801829	0.452437
C	1.767643	0.539358	0.123990
N	0.632700	-1.695335	-0.667145
H	-1.253225	2.136490	-0.227800
F	-2.409089	-0.207335	0.173267
H	2.813121	0.805323	0.235194
H	1.737070	-1.366380	1.266891
H	1.186483	2.503642	-0.402736

TS(3'→4'): B3LYP/6-311+G(2d,p) (*E* = -385.610075; ZPVE = 0.081778)

C	0.728872	1.513051	-0.201461
C	-0.643185	1.233212	-0.268334
C	-1.130223	-0.044449	-0.037045
C	-0.180139	-1.019472	-0.157342
C	1.482480	-0.761365	0.415075
C	1.677172	0.611616	0.295038
N	0.820674	-1.540433	-0.674046
H	-1.351683	2.036253	-0.440621
F	-2.394819	-0.294866	0.365363
H	2.564008	1.023810	0.768059
H	1.034953	2.539304	-0.361542
H	1.951510	-1.358095	1.188578

4': B3LYP/6-311+G(2d,p) (*E* = -385.630229; ZPVE = 0.083584)

C	0.560130	1.522957	-0.134380
C	-0.727738	1.187730	-0.409340
C	-1.168197	-0.150628	-0.083590
C	-0.289249	-1.095225	-0.336695
C	1.760042	-0.668904	0.286683
C	1.597650	0.674084	0.422313
N	0.901831	-1.445640	-0.514510
H	-1.404491	1.906830	-0.862865
F	-2.358550	-0.353491	0.528513
H	2.418982	1.197579	0.900846
H	0.864764	2.544852	-0.340765
H	2.639049	-1.168443	0.677797

^{1}A"-**2'**: CASSCF(8,8)/cc-pVTZ (E=-383.5422261284; ZPVE=0086108)

N	-0.01760804	-0.83889145	0.24078618
C	-0.11205294	-0.01685311	1.20485950
C	0.90793008	0.07362051	2.25326157
C	0.81610024	0.94600564	3.28424668
C	-1.25152099	0.90156025	1.33648264
C	-1.32228720	1.77054965	2.38249660
C	-0.30412790	1.81709552	3.37314510
H	1.59211648	0.96917003	4.02350235
H	-2.16068006	2.43465424	2.46455073
F	1.93391168	-0.74381471	2.14675951
H	-0.37617496	2.50664663	4.18859243
H	-2.01207614	0.85694039	0.58392841

TS(2'→3'): CASSCF(8,8)/cc-pVTZ (E=-383.5281307427; ZPVE=0.085940)

N	0.20420659	0.11507051	-0.06555077
C	0.01481714	0.02059585	1.17050743
C	0.88449013	-0.08143432	2.34275055
C	0.78481919	0.88635486	3.26306915
C	-1.21045542	0.79096359	1.26970720
C	-1.13566267	1.95210469	2.11156535
C	-0.18057960	1.97590423	3.08208418
H	1.44303286	0.89396477	4.10921955
H	-1.87123954	2.73030257	2.04900193
F	1.76609588	-1.05410779	2.40733027
H	-0.13440271	2.79467273	3.77272749
H	-2.05972481	0.52814633	0.68180847

3': CASSCF(8,8)/cc-pVTZ (E=-383.5355428704; ZPVE=0.087813)

N	0.00358762	0.45578957	0.06536839
C	0.05370629	-0.03985459	1.21629882
C	0.93646640	-0.13410291	2.36655307
C	0.81061178	0.88495535	3.22651196
C	-1.17422414	0.69659144	1.16337466
C	-1.11286247	1.90512002	2.00631213
C	-0.16529971	1.96092331	2.97012639
H	1.44897604	0.94695055	4.08582878
H	-1.84092498	2.68823624	1.91339016
F	1.79259193	-1.12067890	2.49904060
H	-0.11432767	2.81445765	3.61824679
H	-2.10796547	0.23653908	0.91249138

TS(3'→4'): CASSCF(8,8)/cc-pVTZ (E=-383.5006782972; ZPVE=0.086226)

N	0.63729614	-0.08385323	-0.26691648
C	0.30175108	-0.17348327	0.93202764
C	0.73702443	-0.10020342	2.23291254
C	1.66134560	0.89548904	2.48422813
C	0.16534744	1.28764927	-0.09915451
C	1.03183889	2.21800470	0.48390180
C	1.85439074	1.95459998	1.58185053
H	2.15765929	0.91381550	3.43552136
H	0.95213157	3.23872924	0.15723279
F	0.18522750	-0.81602520	3.19539666
H	2.55229139	2.71622658	1.87149644
H	-0.72323543	1.56565750	-0.62985033

4': CASSCF(8,8)/cc-pVTZ (E=-383.537097608; ZPVE=0.087999)

N	0.49204755	-0.00768875	-0.22899680
C	0.47170976	-0.44875714	0.94787818
C	0.77184737	-0.16770425	2.20821452
C	1.78373587	0.84668303	2.45373368
C	0.26417568	1.38329411	-0.28195888
C	0.88199216	2.24469328	0.55528128
C	1.79546177	1.94381833	1.66535628
H	2.48925877	0.73168206	3.25530267
H	0.76034218	3.28891659	0.33446485
F	0.12779401	-0.69630444	3.23494792
H	2.52753162	2.70331192	1.87054884
H	-0.32479480	1.73636019	-1.10475194

6. References

S1 K. Kanakarajan, K. Haider and A. W. Czarnik, *Synthesis*, 1988, 566–568.

S2 A. D. Becke, *J. Chem. Phys.*, 1993, **98**, 5648–5652.

S3 A. D. Becke, *Phys. Rev. A*, 1988, **38**, 3098–3100.

S4 C. Lee, W. Yang and R. G. Parr, *Phys. Rev. B*, 1988, **37**, 785–789.

S5 S. H. Vosko, L. Wilk and M. Nusair, *Can. J. Phys.*, 1980, **58**, 1200–1211.

S6 M. J. Frisch, G. W. Trucks, H. B. Schlegel, G. E. Scuseria, M. A. Robb, J. R. Cheeseman, G. Scalmani, V. Barone, G. A. Petersson, H. Nakatsuji, X. Li, M. Caricato, A. V. Marenich, J. Bloino, B. G. Janesko, R. Gomperts, B. Mennucci, H. P. Hratchian, J. V. Ortiz, A. F. Izmaylov, J. L. Sonnenberg, D. Williams-Young, F. Ding, F. Lipparini, F. Egidi, J. Goings, B. Peng, A. Petrone, T. Henderson, D. Ranasinghe, V. G. Zakrzewski, J. Gao, N. Rega, G. Zheng, W. Liang, M. Hada, M. Ehara, K. Toyota, R. Fukuda, J. Hasegawa, M. Ishida, T. Nakajima, Y. Honda, O. Kitao, H. Nakai, T. Vreven, K. Throssell, J. A. Montgomery, Jr., J. E. Peralta, F. Ogliaro, M. J. Bearpark, J. J. Heyd, E. N. Brothers, K. N. Kudin, V. N. Staroverov, T. A. Keith, R. Kobayashi, J. Normand, K. Raghavachari, A. P. Rendell, J. C. Burant, S. S. Iyengar, J. Tomasi, M. Cossi, J. M. Millam, M. Klene, C. Adamo, R. Cammi, J. W. Ochterski, R. L. Martin, K. Morokuma, O. Farkas, J. B. Foresman, and D. J. Fox, *Gaussian 16, Revision B.01*. 2016.

S7 C. M. Nunes, A. K. Eckhardt, I. Reva, R. Fausto, P. R. Schreiner, *J. Am. Chem. Soc.*, 2019, **141**, 14340–14348.

S8 V. Barone, *J. Chem. Phys.*, 2005, **122**, 014108.

S9 J. Bloino and V. Barone, *J. Chem. Phys.*, 2012, **136**, 124108.

S10 Double and triple-ζ basis sets of SNS, are available for download at https://smart.sns.it (accessed July 1, 2021).

S11 T. H. Dunning, *J. Chem. Phys.*, 1989, **90**, 1007–1023.

S12 P. Piecuch, S. A. Kucharski, K. Kowalski and M. Musiał, *Comput. Phys. Commun.*, 2002, **149**, 71–96.

S13 J. L. Bentz, R. M. Olson, M. S. Gordon, M. W. Schmidt and R. A. Kendall, *Comput.*

Phys. Commun., 2007, **176**, 589–600.

S14 R. M. Olson, J. L. Bentz, R. A. Kendall, M. W. Schmidt and M. S. Gordon, *J. Chem. Theory Comput.*, 2007, **3**, 1312–1328.

S15 M. W. Schmidt, K. K. Baldridge, J. A. Boatz, S. T. Elbert, M. S. Gordon, J. H. Jensen, S. Koseki, N. Matsunaga, K. A. Nguyen, S. Su, T. L. Windus, M. Dupuis and J. A. Montgomery, *J. Comput. Chem.*, 1993, **14**, 1347–1363.

S16 P. E. M. Siegbahn, J. Almlöf, A. Heiberg and B. O. Roos, *J. Chem. Phys.*, 1981, **74**, 2384–2396.

S17 K. Ruedenberg, M. W. Schmidt, M. M. Gilbert and S. T. Elbert, *Chem. Phys.*, 1982, **71**, 65–78.

S18 B. O. Roos, P. R. Taylor and P. E. M. Sigbahn, *Chem. Phys.*, 1980, **48**, 157–173.

S19 P. Siegbahn, A. Heiberg, B. Roos and B. Levy, *Phys. Scr.*, 1980, **21**, 323–327.

S20 N. P. Gritsan, A. D. Gudmundsdóttir, D. Tigelaar, Z. Zhu, W. L. Karney, C. M. Hadad and M. S. Platz, *J. Am. Chem. Soc.*, 2001, **123**, 1951–1962.

S21 W. L. Karney and W. T. Borden, *J. Am. Chem. Soc.*, 1997, **119**, 1378–1387.

S22 K. Hirao, *Chem. Phys. Lett.*, 1993, **201**, 59–66.

S23 K. Hirao, *Int. J. Quantum Chem.*, 1992, **44**, 517–526.

S24 K. Hirao, *Chem. Phys. Lett.*, 1992, **196**, 397–403.

S25 K. Hirao, *Chem. Phys. Lett.*, 1992, **190**, 374–380.

S26 C. M. Nunes, I. Reva, R. Fausto, In *Tunnelling in Molecules: Nuclear Quantum Effects from Bio to Physical Chemistry*; S. Kozuch, J. Kästner, Eds.; Royal Society of Chemistry, 2021; pp 1–60.

S27 L. Brillouin, *Compt. Rend. Hebd. Seances Acad. Sci.*, 1926, **183**, 24–26.

S28 G. Wentzel, *Zeitschrift für Phys.*, 1926, **38**, 518–529.

S29 H. A. Kramers, *Zeitschrift für Phys.*, 1926, **39**, 828–840.

S30 W. T. Borden, *WIREs Comput. Mol. Sci.*, 2016, **6**, 20–46.

S31 G. A. Zhurko, *ChemCraft*, *Version 1.8*. http://www.chemcraftprog.com, 2016.